# New Type of Spectral-Domain Analysis of a Microstrip Line

KAZUNORI UCHIDA, MEMBER, IEEE, TAKEAKI NODA, MEMBER, IEEE, AND TOSHIAKI MATSUNAGA

*Abstract* —The problem of an open microstrip line is analyzed by the spectral-domain method combined with the sampling theorem. In the spectral domain, the boundary conditions of zero tangential electric fields are expressed in terms of the convolution integral forms with a sampling function, and these relations are discretized by the method of moments with the spherical Bessel function as a weighting function. A well-chosen incorporation of the Weber–Schafheitlin integration formula yields good accuracy and saves a significant amount of time in numerical calculations. Numerical examples are shown for the effective dielectric constants and for the current distributions, both longitudinal and transverse, in comparison with the results obtained by various other methods.

## I. Introduction

MICROSTRIP has become one of the most important elements in microwave integrated circuits, and a great many authors have analyzed the propagation characteristics of modes on a microstrip line. Earlier works [1], [2] were based on the quasi-TEM approximation, which is valid only for low frequencies. For high frequencies, however, a rigorous treatment or a full-wave analysis is needed to account for the dispersive properties of the propagation characteristics of the stripline [3]–[13]. In this case the accuracy of the final results depends on how accurately the current distributions on the microstrip line have been evaluated.

Various methods based on a full-wave theory have been proposed to obtain both longitudinal and transverse current distributions. The spectral-domain approach seems to be one of the most powerful analytical methods, since the Green function in the spectral domain can be obtained rigorously for a microstrip-like structure. In the conventional spectral-domain analyses [5], [11], however, the Galerkin's procedure has been applied in order to determine the unknown coefficients of the expanded current distributions, and the final numerical results are strongly dependent on the choice of the basis functions. To overcome this situation, Kobayashi [9] has proposed simple but accurate closed-form expressions for the current distributions to be used as the basis functions. However, the closed-form expressions do not necessarily reveal the frequency dependence of the current distributions with good accuracy [12].

Manuscript received August 30, 1988; revised January 12, 1989.
The authors are with the Department of Communication and Computer Engineering, Fukuoka Institute of Technology, 3-30-1, Wajiro-Higashi, Higashi-ku, Fukuoka, 811-02 Japan.
IEEE Log Number 8927165.

In this paper, we propose a new type of spectral-domain method to solve the current distributions on the microstrip line rigorously. The key point of the present method is the band limitation of the spectral functions through convolution integration with a sampling function. Since all the boundary conditions are satisfied in the spectral domain, Fourier inverse transformation is not required to solve surface current distributions. In this respect our method differs from the space-domain approach [13]. This new method has been successfully applied to the plane wave scattering by metallic gratings where discretization was performed by using a point matching method for the numerical calculations. In contrast to this, discretization in the present method is performed by the method of moments using the spherical Bessel function as a weighting function. The main advantage of the present method is that the Weber–Schafheitlin integration formula can be effectively incorporated into the numerical integrations, which enables us not only to save much computation time but also to obtain accurate numerical results.

## II. Formulation of the Problem

Fig. 1 shows the geometry of the problem, where it is assumed that the thickness of the strip is negligibly small, the dielectric is lossless, and the strip as well as the ground plane is perfectly conducting. In the following analysis, the time dependence $\exp(j\omega t)$ is considered and this factor will be suppressed throughout this paper. The boundary conditions of the present problem are summarized as follows:

(B1) Radiation condition.

(B2) Continuity of tangential electric fields:

$$E_x(x,h+0,z)=E_x(x,h-0,z)$$
$$E_z(x,h+0,z)=E_z(x,h-0,z). \qquad (1)$$

(B3) Continuity of tangential magnetic fields and their discontinuity on the strip:

$$H_x(x,h+0,z)-H_x(x,h-0,z)=-\sqrt{\epsilon_0/\mu_0}\,\tilde{J}_z(x,z)$$
$$H_z(x,h+0,z)-H_z(x,h-0,z)=\sqrt{\epsilon_0/\mu_0}\,\tilde{J}_x(x,z) \qquad (2)$$

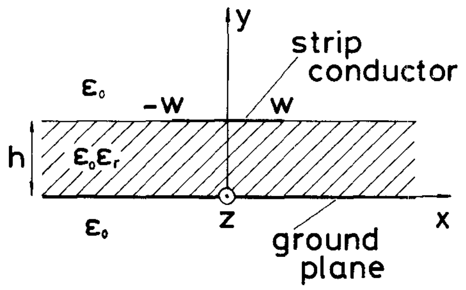

Fig. 1. Geometry of the problem.

where $\tilde{J}_z(x, z)$ and $\tilde{J}_x(x, z)$ are normalized surface currents on the strip.

(B4) Perfect conductor condition on the ground plane:

$$E_x(x,0,z) = E_z(x,0,z) = 0. \quad (3)$$

(B5) Perfect conductor condition on the strip:

$$E_x(x,h,z) = E_z(x,h,z) = 0. \quad (4)$$

We designate the propagation constant by $\beta$, and we express the $z$ dependence of the fields as follows:

$$E(x,y,z) = E(x,y)\exp(-j\beta z). \quad (5)$$

In the subsequent analysis, this exponential factor will also be omitted.

Analytical discussions are based on the following Fourier transformation pair:

$$f(\zeta) = \int_{-\infty}^{\infty} f(x)\exp(j\zeta x)\,dx$$

$$f(x) = (1/2\pi)\int_{-\infty}^{\infty} f(\zeta)\exp(-j\zeta x)\,d\zeta. \quad (6)$$

After straightforward but somewhat lengthy algebraic manipulations, we obtain the Fourier transforms of the tangential electric fields at $y = h$ as follows:

$$E_x(\zeta,h) = U_1(\zeta,\beta)\tilde{J}_x(\zeta) + U_2(\zeta,\beta)\tilde{J}_z(\zeta)$$

$$E_z(\zeta,h) = U_2(\beta,\zeta)\tilde{J}_x(\zeta) + U_1(\beta,\zeta)\tilde{J}_z(\zeta) \quad (7)$$

where $\tilde{J}_x(\zeta)$ and $\tilde{J}_z(\zeta)$ are the Fourier transforms of the surface current on the strip described in (2), and where other spectral functions used are defined by

$$U_1(\zeta,\beta) = [kg_0(\zeta)\tan(kh) - \gamma g_1(\zeta)]/\kappa_0\Delta(\zeta,\beta)$$

$$U_2(\zeta,\beta) = -[k\tan(kh) - \gamma]\zeta\beta/\kappa_0\Delta(\zeta,\beta) \quad (8)$$

with

$$g_i(\zeta) = \kappa_i^2 - \zeta^2 \qquad (i = 0.1) \quad (9)$$

$$\Delta(\zeta,\beta) = -j[\gamma + k\cot(kh)][\epsilon_r\gamma - k\tan(kh)] \quad (10)$$

$$\gamma = \sqrt{\zeta^2 + \beta^2 - \kappa_0^2} \qquad k = \sqrt{\kappa_1^2 - \zeta^2 - \beta^2}$$

$$\kappa_0 = \omega\sqrt{\epsilon_0\mu_0} \qquad \kappa_1 = \omega\sqrt{\epsilon_1\mu_0} = \kappa_0\sqrt{\epsilon_r}. \quad (11)$$

In the above expressions, we have assumed an $\exp(-\gamma y)$ dependence for $y > h$ corresponding to the boundary condition (B1). In addition, it should be noted that these spectral expressions satisfy the boundary conditions (B2)–(B4).

Now we let the remaining boundary condition (B5) be satisfied in the spectral domain in the following manner. Since the Fourier transform corresponding to a finite section in the space domain is obtained from the convolution integration with a sampling function in the spectral domain, the boundary conditions for (B5) are rewritten in the spectral domain as follows:

$$(1/\pi)\int_{-\infty}^{\infty} E_x(t,h)S(t-\zeta)\,dt = 0$$

$$(1/\pi)\int_{-\infty}^{\infty} E_z(t,h)S(t-\zeta)\,dt = 0 \quad (12)$$

where the sampling function is defined by

$$S(\zeta) = \sin(\zeta w)/\zeta. \quad (13)$$

As a result, the problem is reduced to finding the unknown surface currents so that (12) may be satisfied in the $\zeta$ plane.

## III. Discretization

Now we recall that the sampling function defined by (13) is a reproducing kernel for any entire functions to order $w$ [15]. Since the spherical Bessel function has this analytical property, we have

$$(1/\pi)\int_{-\infty}^{\infty} j_\mu(\zeta w)S(t-\zeta)\,d\zeta = j_\mu(tw) \quad (14)$$

where the spherical Bessel function can be expressed in terms of the Bessel function of half-integer order as follows:

$$j_\mu(x) = \sqrt{\pi/2x}\,J_{\mu+1/2}(x). \quad (15)$$

Multiplying by $j_\mu(\zeta w)$ in (12) and integrating with respect to $\zeta$ from $-\infty$ to $\infty$ leads to

$$(1/\pi)\int_{-\infty}^{\infty} E_x(t,h)j_\mu(tw)\,dt = 0$$

$$(1/\pi)\int_{-\infty}^{\infty} E_z(t,h)j_\mu(tw)\,dt = 0 \quad (16)$$

$$(\mu = 0,1,2,3,\cdots).$$

Taking into account the singularities of the surface currents near the edges of the strip, we expand them in the form

$$J_x(x) = \sum_{\nu=0}^{\infty} A_\nu\Phi_\nu(x)$$

$$J_z(x) = \sum_{\nu=0}^{\infty} B_\nu\Psi_\nu(x) \quad (17)$$

where $A_\nu$ and $B_\nu$ are unknown coefficients to be solved and

$$\Phi_\nu(x) = \cos[(\nu+1)\phi]/[(\nu+1)\pi w] \qquad (\nu \text{ even})$$

$$= -j\sin[(\nu+1)\phi]/[(\nu+1)\pi w] \qquad (\nu \text{ odd})$$

$$\Psi_\nu(x) = \cos(\nu\phi)/\left[\pi\sqrt{w^2-x^2}\right] \qquad (\nu \text{ even})$$

$$= -j\sin(\nu\phi)/\left[\pi\sqrt{w^2-x^2}\right] \qquad (\nu \text{ odd})$$

$$(18)$$

where

$$\phi = \sin^{-1}(x/w). \tag{19}$$

The Fourier transforms of (17) are given as follows [16]:

$$\tilde{J}_x(\zeta) = \sum_{\nu=0}^{\infty} A_\nu J_{\nu+1}(\zeta w)/\zeta w$$

$$\tilde{J}_z(\zeta) = \sum_{\nu=0}^{\infty} B_\nu J_\nu(\zeta w) \tag{20}$$

where $J_\nu(x)$ is the Bessel function.

Combining (7), (16), and (20), equations (16) can be rearranged in the following matrix forms:

$$\sum_{\nu=0}^{\infty} [A_\nu K_1(\beta;\nu,\mu) + B_\nu K_2(\beta;\nu,\mu)] = 0$$

$$\sum_{\nu=0}^{\infty} [A_\nu K_3(\beta;\nu,\mu) + B_\nu K_4(\beta;\nu,\mu)] = 0 \tag{21}$$

$$(\mu = 0,1,2,3,\cdots)$$

where

$$\begin{aligned} K_1(\beta;\nu,\mu) &= 2\int_0^\infty U_1(t,\beta)[J_{\nu+1}(tw)/tw]\, j_\mu(tw)\, dt \\ &\qquad (\mu+\nu \text{ even}) \\ &= 0 \qquad (\mu+\nu \text{ odd}) \end{aligned}$$

$$\begin{aligned} K_2(\beta;\nu,\mu) &= 0 \qquad (\mu+\nu \text{ even}) \\ &= 2\int_0^\infty U_2(t,\beta) J_\nu(tw)\, j_\mu(tw)\, dt \\ &\qquad (\mu+\nu \text{ odd}) \end{aligned}$$

$$\begin{aligned} K_3(\beta;\nu,\mu) &= 0 \qquad (\mu+\nu \text{ even}) \\ &= 2\int_0^\infty U_2(\beta,t)[J_{\nu+1}(tw)/tw]\, j_\mu(tw)\, dt \\ &\qquad (\mu+\nu \text{ odd}) \end{aligned}$$

$$\begin{aligned} K_4(\beta;\nu,\mu) &= 2\int_0^\infty U_1(\beta,t) J_\nu(tw)\, j_\mu(tw)\, dt \\ &\qquad (\mu+\nu \text{ even}) \\ &= 0 \qquad (\mu+\nu \text{ odd}). \end{aligned} \tag{22}$$

The propagation constant $\beta$ of the stripline mode is solved in such a way that the determinant of (21) becomes zero, and the unknown coefficients of the expanded surface currents can also be determined as an eigenvector.

In general, we have to resort to numerical matrix calculations by truncating $\mu$ and $\nu$ in (21) appropriately. In this case it is important to carry out the numerical integrations precisely but without much computation time. We propose here an efficient numerical method based on the Weber–Schafheitlin integration formula as shown in the Appendix. The numerical method proposed here has two merits. One is that it saves computation considerably; the other is that the numerical results of the current distributions can be obtained with good accuracy. This is why the method greatly accelerates the convergence of the inner product integrations, especially for large $\mu$ and $\nu$.

## IV. TEM Mode

In the preceding section we have derived the equation for the propagation constant of a hybrid mode as well as for the current distributions. It is not so easy to solve the equation numerically, since it requires integration over a semi-infinite interval. For $\epsilon_r = 1$, however, we can proceed with more analytical discussions. When the dielectric slab is replaced by free space ($\epsilon_r = 1$), the microstrip line supports a TEM wave with propagation constant $\kappa_0$. In this case the following relations are satisfied:

$$U_1(\kappa_0,\zeta) = 0 \tag{23}$$

$$\tilde{J}_x(x,z) = 0 \qquad (A_\nu = 0). \tag{24}$$

Consequently, (22) is reduced to

$$\sum_{\nu=0}^{\infty} B_\nu K_2(\kappa_0;\nu,\mu) = 0 \tag{25}$$

where

$$\begin{aligned} K_2(\kappa_0;\nu,\mu) &= j\int_0^\infty (1-e^{-2ht}) J_\nu(tw)\, j_\mu(tw)\, dt \qquad (\mu+\nu \text{ odd}) \\ &= 0 \qquad (\mu+\nu \text{ even}). \end{aligned} \tag{26}$$

The above integrations can be performed analytically. The first term is given by the Weber-Schafheitlin integration formula (see the Appendix). As for the second term, we have, for $2h > w$,

$$\begin{aligned} &\int_0^\infty e^{-2ht} J_\nu(tw)\, j_\mu(tw)\, dt \\ &= (\sqrt{\pi}/w) \sum_{m=0}^{\infty} (-1)^m \Gamma(2M+2m) \\ &\quad \cdot F(M+m, M-\nu-m, \mu+3/2; X) \\ &\quad /[\Gamma(m+1)\Gamma(\nu+1+m)\Gamma(\mu+3/2)2^{2M+2m}X^{M+m}] \end{aligned} \tag{27}$$

TABLE I
COEFFICIENTS OF CURRENT DISTRIBUTIONS

| | 1 GHz | 10 GHz | 20 GHz |
|---|---|---|---|
| $A_1$ | $1.60\times10^{-3}$ | $6.90\times10^{-3}$ | $1.68\times10^{-1}$ |
| $A_3$ | $1.97\times10^{-5}$ | $-1.32\times10^{-3}$ | $-1.47\times10^{-2}$ |
| $A_5$ | $-1.46\times10^{-8}$ | $-3.21\times10^{-5}$ | $3.87\times10^{-4}$ |
| $A_7$ | $-5.62\times10^{-9}$ | $-6.75\times10^{-6}$ | $-6.43\times10^{-5}$ |
| $A_9$ | $2.75\times10^{-9}$ | $3.05\times10^{-6}$ | $2.05\times10^{-6}$ |
| $B_0$ | 1.00 | 1.00 | 1.00 |
| $B_2$ | $3.13\times10^{-2}$ | $1.11\times10^{-1}$ | $2.50\times10^{-1}$ |
| $B_4$ | $4.72\times10^{-4}$ | $2.96\times10^{-3}$ | $1.06\times10^{-2}$ |
| $B_6$ | $5\ 92\times10^{-6}$ | $2.96\times10^{-5}$ | $-2.08\times10^{-4}$ |
| $B_8$ | $1.79\times10^{-8}$ | $1.41\times10^{-6}$ | $1.14\times10^{-5}$ |

$\epsilon_r=11.7$; $h=3.04$ mm, $2w=3.17$ mm.

where

$$M=(\mu+\nu+1)/2$$
$$X=1/(1+H^2)$$
$$H=2h/w. \tag{28}$$

$F(\alpha,\beta,\gamma;z)$ is the Gauss hypergeometric function, defined by

$$F(\alpha,\beta,\gamma;z)=\Gamma(\gamma)/[\Gamma(\alpha)\Gamma(\beta)]$$
$$\cdot\sum_{n=0}^{\infty}\Gamma(\alpha+n)\Gamma(\beta+n)z^n/[\Gamma(\gamma+n)\Gamma(n+1)]. \tag{29}$$

As a result, we can evaluate the surface currents precisely without any numerical integrations for a TEM wave. Moreover, it can be easily proved from the above integration formulas that when $H\to\infty$, the expansion coefficients $B_\nu$ should be zero except for $\nu=0$. Thus we have

$$\tilde{J}_z(x)=B_0/\left[\pi\sqrt{w^2-x^2}\right]\qquad(H\to\infty) \tag{30}$$

which is the Maxwell distribution when $h\to\infty$.

## V. NUMERICAL RESULTS

In the following numerical examples, normalization with regard to the amplitudes of the currents has been made such that $B_0=1.0$, which means that the total longitudinal current is unity; that is,

$$\int_{-w}^{w}\tilde{J}_z(x)\,dx=1. \tag{31}$$

Table I shows numerical examples for the coefficients of the expanded current distributions given by (20). It is found that all terms of the transverse current as well as the higher terms of the longitudinal current are negligibly small for low frequency. This reflects the fact that for low frequencies, the Maxwell distribution given by (30) might be a good approximation for the longitudinal current distribution, neglecting the transverse current.

Table II shows a comparison of effective dielectric constants obtained by three different methods; closed forms for the current distributions have been used in [11], and the variational conformal mapping technique has been employed in [12]. Some discrepancies within 0.6 percent have been observed in the numerical results of the three different methods, and the present results are more in agreement with the variational conformal mapping technique than with the closed-form expression.

Table III shows another example of the effective dielectric constant in comparison with the iteration method [4], the closed-form expression [11], and the present method. The matrix sizes used are (20×20), (2×2), and (6×6), respectively. As far as the matrix size is concerned, the closed-form expression is better than others. However, the upper limit of numerical integration has been chosen as $\alpha_u=1.5\times10^3/w$ in [11], whereas $\alpha_u=50.0/w$ in the present method. Thus the present method saves much computation time in the numerical integrations.

Fig. 2 shows the current distributions for three different frequencies: $f=1$, 10, and 20 GHz; the parameters used are $h=3.04$ mm, $2w=3.17$ mm, and $\epsilon_r=11.7$. It is demonstrated that the amplitude of the transverse current changes more rapidly as a function of frequency than the longitudinal current. Fig. 3 is another version of Fig. 2, where the longitudinal current has been normalized as

TABLE II
EFFECTIVE DIELECTRIC CONSTANT

| | REFERENCE [11] | REFERENCE [12] | PRESENT METHOD |
|---|---|---|---|
| 2 | 1.64667 | 1.64721 | 1.64677 |
| 4 | 2.91642 | 2.91690 | 2.91677 |
| 8 | 5.44034 | 5.44052 | 5.44116 |
| 16 | 10.4789 | 10.4786 | 10.4807 |
| 128 | 80.9729 | 80.9649 | 80.9903 |
| $\varepsilon_r$ | $h/\lambda=0.0$ | $2w/h=1.0$ | |
| 2 | 1.728 | 1.730 | 1.7282 |
| 4 | 3.317 | 3.319 | 3.3178 |
| 8 | 6 742 | 6.753 | 6.7530 |
| 16 | 14.01 | 14.08 | 14.082 |
| 128 | 123.6 | 124.2 | 124.26 |
| $\varepsilon_r$ | $h/\lambda=0.1$ | $2w/h=1.0$ | |
| 2 | 1.966 | 1.969 | 1.9687 |
| 4 | 3.953 | 3.956 | 3.9599 |
| 8 | 7.945 | 7.948 | 7.9555 |
| 16 | 15.94 | 15.95 | 15.953 |
| 128 | 127.9 | 127.9 | 127.95 |
| $\varepsilon_r$ | $h/\lambda=1.0$ | $2w/h=1.0$ | |

TABLE III
EFFECTIVE DIELECTRIC CONSTANT

| | REFERENCE [4] | REFERENCE [11] | PRESENT METHOD |
|---|---|---|---|
| A | | 6.51914 | |
| B | 6.51912 | 6.51941 | 6.51920 |

$\varepsilon_r=9.7$, $h=1.27$mm, $2w=1.219$mm, $f=1$GHz
A: USING ONLY $J_z(x)$
B: USING BOTH $J_z(x)$ AND $J_x(x)$

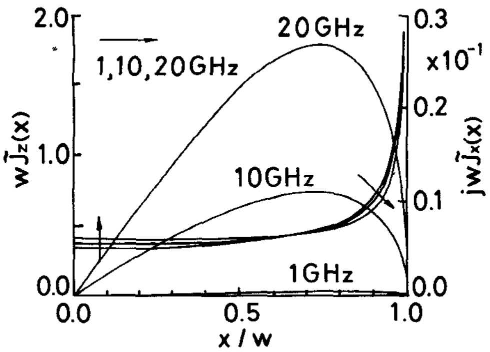


Fig. 2. Current distributions versus normalized distance with the frequency as a parameter ($h = 3.04$ mm, $2w = 3.17$ mm, and $\epsilon_r = 11.7$).

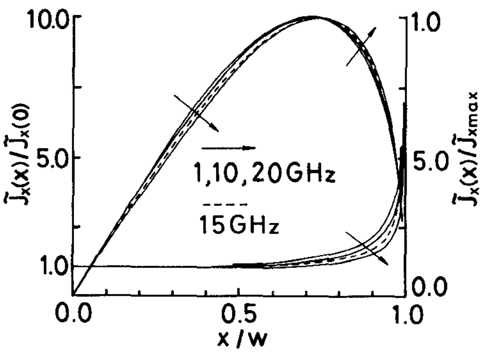


Fig. 3. Normalized current distributions versus normalized distance with frequency as a parameter ($h = 3.04$ mm, $2w = 3.17$ mm, and $\epsilon_r = 11.7$). ---- Shin, Wu, Jeng and Chen [12]; ———— present method.

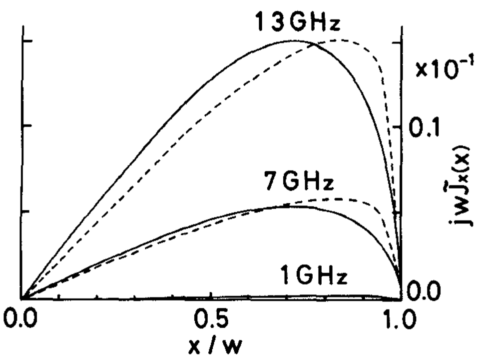


Fig. 4. Transverse current distributions versus normalized distance with frequency as a parameter ($h = 3.04$ mm, $2w = 3.17$ mm, and $\epsilon_r = 11.7$). ---- Faché and De Zutter [13]; ———— present method.

$\tilde{J}_z(x)/\tilde{J}_z(0)$ and the transverse current as $\tilde{J}_x(x)/\tilde{J}_{x\max}$, where $\tilde{J}_{x\max}$ is its maximum amplitude at a certain point. The normalization helps us to investigate the frequency characteristics of the current distributions. In Fig. 3 comparison has also been made with the results based on the variational conformal mapping technique [12].

Fig. 4 shows the transverse current distributions in comparison with the results of the space-domain method starting from the calculation of a dyadic Green's function in the spectral domain [13]. As for the maximum points, considerable discrepancies are observed between these two results. The main reason for the discrepancies might be the different choice of basis functions in the two methods; the functions (18) are used in the present method, while the elementary triangular functions are used in the space-domain method [13]. It should be noted that if we choose only one basis function ($\nu = 1$) in the present method, the maximum value always occurs at $x/w = 1/\sqrt{2}$.

## VI. Conclusion

We have proposed a new type of spectral-domain method combined with the sampling theorem in order to evaluate the current distributions on a microstrip line accurately. Discretization for numerical calculations has been performed by the method of moments using the spherical Bessel function as a weighting function for which the sampling function is a reproducing kernel. Since the Weber-Schafheitlin integration formula can be incorporated into the present formulations, good accuracy as well as a considerable saving of computation time has been achieved. The results also show good convergence. Numerical calculations have been carried out for the effective dielectric constants and the current distributions in comparison with various other methods. It has been demonstrated that the present method is very effective in analyzing an open microstrip line.

The present method can easily be applied to more complicated structures such as a multilayered stripline and a multistrip line. This will be the subject of future work.

## Appendix
## Computation of the Integrations of (22)

For $t \gg \kappa_0$, we have the following asymptotic relations from (8)–(10):

$$\begin{aligned} U_1(t,\beta) &\sim t/[\kappa_0(\epsilon_r+1)] = \tilde{U}_1 t \\ U_2(t,\beta) &= U_2(\beta,t) \sim -\beta/[\kappa_0(\epsilon_r+1)] = \tilde{U}_2 \\ U_1(\beta,t) &\sim [(\epsilon_r+1)\kappa_0 - 2\beta]/[2\kappa_0(\epsilon_r+1)t] = \tilde{U}_3/t. \end{aligned} \tag{A1}$$

By extracting these main terms in (22), we can rewrite the equations in the following forms:

$$\begin{aligned} K_1(\beta;\nu,\mu) &= 2\int_0^\infty [U_1(t,\beta) - \tilde{U}_1 t] \\ &\quad \cdot [J_{\nu+1}(tw)/tw]\, j_\mu(tw)\, dt \\ &\quad + (2/w)\tilde{U}_1 \int_0^\infty J_{\nu+1}(tw)\, j_\mu(tw)\, dt \\ K_2(\beta;\nu,\mu) &= 2\int_0^\infty [U_2(t,\beta) - \tilde{U}_2]\, J_\nu(tw)\, j_\mu(tw)\, dt \\ &\quad + 2\tilde{U}_2 \int_0^\infty J_\nu(tw)\, j_\mu(tw)\, dt \\ K_3(\beta;\nu,\mu) &= 2\int_0^\infty [U_2(\beta,t) - \tilde{U}_2][J_{\nu+1}(tw)/tw]\, j_\mu(tw) dt \\ &\quad + (2/w)\tilde{U}_2 \int_0^\infty t^{-1} J_{\nu+1}(tw)\, j_\mu(tw)\, dt \\ K_4(\beta;\nu,\mu) &= 2\int_0^\infty [U_1(\beta,t) - \tilde{U}_3/t]\, J_\nu(tw)\, j_\mu(tw)\, dt \\ &\quad + 2\tilde{U}_3 \int_0^\infty t^{-1} J_\nu(tw)\, j_\mu(tw)\, dt. \end{aligned} \tag{A2}$$

In the above expressions, the integrands of the first terms are so rapidly convergent that numerical integration over a finite interval is enough to obtain good accuracy. On the other hand, the second terms are calculated analytically by means of the Weber-Schafheitlin formula as follows [16]:

$$\int_0^\infty t^{-m} J_n(tw)\, j_\mu(tw)\, dt = (\sqrt{\pi}/2w)(w/2)^m \Gamma(m+1/2)\Gamma[(\mu+n-m+1)/2] \Big/ \{\Gamma[(m+\mu-n+2)/2]\Gamma[(m-\mu+n+1)/2] \cdot \Gamma[(m+\mu+n+2)/2]\} \qquad \text{(A3)}$$

$$(m=0 \text{ or } 1, \quad n=\nu \text{ or } \nu+1)$$

where $\Gamma(x)$ is the Gamma function.

It is worth noting that the above integration is divergent in the special case of $m=0$ and $n=\mu=0$, which corresponds to $\mu=\nu=0$ in the last expression of (A2). In this case, we put

$$\tilde{U}_3/t \to \tilde{U}_3 t \Big/ \left[t^2+(\alpha/w)^2\right] \qquad \text{(A4)}$$

where $\alpha$ is an arbitrary real number. Then, the following integration formula is applicable [16]:

$$\int_0^\infty \left\{t \Big/ \left[t^2+(\alpha/w)^2\right]\right\} J_0(tw)\, j_0(tw)\, dt = \sinh\alpha K_0(\alpha)/\alpha \qquad \text{(A5)}$$

where $K_0(x)$ is the modified Bessel function.

## References


[1] H. A. Wheeler, "Transmission-line properties of parallel strips separated by a dielectric sheet," *IEEE Trans. Microwave Theory Tech.*, vol. MTT-13, pp. 172–185, Mar. 1965.

[2] E. Yamashita and R. Mittra, "Variational method for the analysis of microstrip lines," *IEEE Trans. Microwave Theory Tech.*, vol. MTT-16, pp. 251–256, Apr. 1968.

[3] E. J. Denlinger, "A frequency dependent solution for microstrip transmission lines," *IEEE Trans. Microwave Theory Tech.*, vol. MTT-19, pp. 30–39, Jan. 1971.

[4] Y. Fujiki, Y. Hayashi, and M. Suzuki, "Analysis of strip transmission lines by iteration method," *Trans. IECE Japan*, vol. 55-B, pp. 212–219, May 1972.

[5] T. Itoh and R. Mittra, "Spectral-domain approach for calculating the dispersion characteristics of microstriplines," *IEEE Trans. Microwave Theory Tech.*, vol. MTT-21, pp. 496–499, July 1973.

[6] E. Yamashita and K. Atsuki, "Analysis of microstrip-like transmission lines by nonuniform discretization of integral equations," *IEEE Trans. Microwave Theory Tech.*, vol. MTT-24, pp. 195–200, Apr. 1976.

[7] E. F. Kuester and D. C. Chang, "Theory of dispersion in microstrip of arbitrary width," *IEEE Trans. Microwave Theory Tech.*, vol. MTT-28, pp. 259–265, Mar. 1980.

[8] E. F. Kuester and D. C. Chang, "Closed-form expressions for the current distribution on parallel strips or microstrip," *IEEE Trans. Microwave Theory Tech.*, vol. MTT-28, pp. 259–265, Mar. 1980.

[9] M. Kobayashi, "Longitudinal and Transverse current distributions on microstriplines and their closed-form expression," *IEEE Trans. Microwave Theory Tech.*, vol. MTT-33, pp. 784–788, Sept. 1985.

[10] M. Hashimoto, "A rigorous solution for dispersive microstrip," *IEEE Trans. Microwave Theory Tech.*, vol. MTT-33, pp. 1131–1137, Nov. 1985.

[11] M. Kobayashi and F. Ando, "Dispersion characteristics of open microstrip lines," *IEEE Trans. Microwave Theory Tech.*, vol. MTT-35, pp. 101–105, Feb. 1987.

[12] C. Shin, R. B. Wu, S. K. Jeng, and C. H. Chen, "A full-wave analysis of microstrip lines by variational conformal mapping technique," *IEEE Trans. Microwave Theory Tech.*, vol. 36, pp. 576–581, Mar. 1988.

[13] N. Faché and D. De Zutter, "Rigorous full-wave space-domain solution for dispersive microstrip lines," *IEEE Trans. Microwave Theory Tech.*, vol. 36, pp. 731–737, Apr. 1988.

[14] K. Uchida, T. Noda, and T. Matsunaga, "Spectral domain analysis of electromagnetic wave scattering by an infinite plane metallic grating," *IEEE Trans. Antennas Propagat.*, vol. AP-35, pp. 46–52, Jan. 1987.

[15] R. B. Young, *An Introduction to Nonharmonic Fourier Series.* New York: Academic Press, 1980.

[16] Moriguchi, Udagawa, and Ichimatsu, *Mathematical Formulae III.* Tokyo: Iwanami Co., 1977.


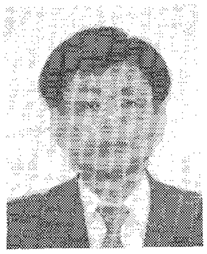


**Kazunori Uchida** (M'83) was born in Fukuoka, Japan, on March 2, 1945. He received the B.E., M.E., and D.E. degrees from Kyushu University in 1967, 1970, and 1974, respectively.

From 1973 to 1975, he was a Research Associate of Computer Science and Communication Engineering at Kyushu University. From 1975 to 1982, he was an Associate Professor at the Fukuoka Institute of Technology (F.I.T.), Fukuoka, Japan. Since 1982 he has been a Professor in the Department of Communication and Computer Engineering at F.I.T. His main interest is electromagnetic field theory.

Dr. Uchida is a member of the Institute of Electronics, Information and Communication Engineers of Japan and the Institute of Television Engineers of Japan.


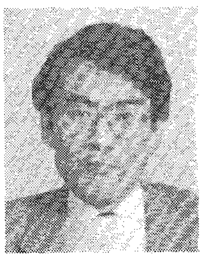


**Takeaki Noda** (M'88) was born in China on October 11, 1942. He graduated from the Fukuoka Junior College of Technology in 1964.

From 1964 to 1969, he was an assistant engineer at the Fukuoka Institute of Technology (F.I.T.), Fukuoka, Japan. Since 1969 he has been a Research Associate in the Department of Communication and Computer Engineering at F.I.T. His main interest is electromagnetic field theory.

Mr. Noda is a member of the Institute of Electronics, Information and Communication Engineers of Japan.



**Toshiaki Matsunaga** was born in Fukuoka, Japan, on October 30, 1941. He graduated from the Fukuoka Junior College of Technology in 1962.

From 1963 to 1967, he was an assistant engineer at the Fukuoka Institute of Technology (F.I.T.), Fukuoka, Japan. From 1967 to 1983, he was a Research Associate at F.I.T., and since 1983 he has been an Assistant Professor in the Department of Communication and Computer Engineering there. His main interest is microwave simulation of electromagnetic wave propagation in tunnels.

Mr. Matsunaga is a member of the Institute of Electronics, Information and Communication Engineers of Japan.